



**POLITECNICO**  
MILANO 1863

SCUOLA DI INGEGNERIA INDUSTRIALE  
E DELL'INFORMAZIONE

EXECUTIVE SUMMARY OF THE THESIS

## Operando X-ray spectroscopic investigation of ceria in redox conditions

LAUREA MAGISTRALE IN ENGINEERING PHYSICS- INGEGNERIA FISICA

Author: SIMONA SORRENTINO

Advisor: PROF. GIACOMO CLAUDIO GHIRINGHELLI

Co-advisor: DR. VINOD K. PAIDI, DR. PIETER GLATZEL

Academic year: 2021-2022

### 1. Introduction

Cerium dioxide ( $\text{CeO}_2$ ), commonly known as ceria, has long been the subject of a multitude of studies in the last decades, due to its peculiar redox properties that make it a promising material in the catalysis and biomedicine fields. In fact, through Ce double oxidation state  $\text{Ce}^{4+}$  and  $\text{Ce}^{3+}$ , ceria is able to store and release O atoms in the lattice, *i.e.* the so-called oxygen storage capacity (OSC). Moreover, studies concerning nanosized-ceria have highlighted how new properties arise at the nanoscale, opening new possibilities in biomedical applications [1]. However, the microscopic basis of OSC and its resulting redox properties have not yet been fully elucidated, and further research is needed to gain a comprehensive understanding of nanoceria behavior in order to make its industrial application predictable. For this purpose, synchrotron radiation is often implemented to retrieve precious information about the electronic structure and the oxidation state of the samples, thanks to the high energy resolution achievable. Therefore, we studied at the European Synchrotron Radiation Facility (ESRF, Grenoble)  $\text{CeO}_2$  nanocrystallites under reducing and oxidizing conditions, together with ceria with the addition of a small percentage of Pt nanopar-

ticles on top (1%Pt/ $\text{CeO}_2$  and 5%Pt/ $\text{CeO}_2$ ), since it is known in literature that the presence of a noble metal enhances ceria chemical activity, making it observable at lower temperatures. The purpose of this study is to acquire X-ray absorption near-edge spectra (XANES) of cerium at the  $L_3$  edge under hydrogen and oxygen gas flow in order to reduce and re-oxidize the sample, respectively. We anticipate the formation of oxygen vacancies when ceria is reduced, and our goal is to determine the impact of such vacancies on the electronic structure of ceria and the effects of their interaction with the lattice.

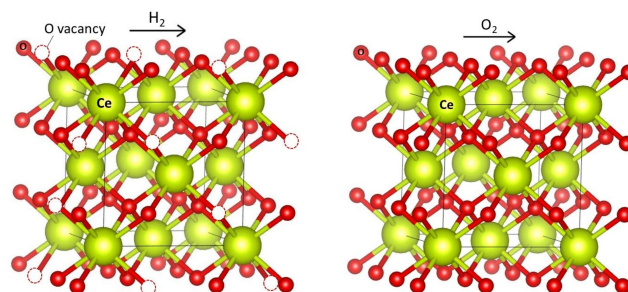


Figure 1: We expect O vacancies to be formed in the  $\text{CeO}_2$  lattice under  $\text{H}_2$  gas flow, and to be re-filled under  $\text{O}_2$ .

## 2. Experimental Techniques

We performed *operando* X-ray absorption spectroscopic measurements at the ID26 beamline (ESRF, Grenoble), exploiting the High Energy Resolution Fluorescence Detected (HERFD) technique to acquire high-resolution spectra at the  $L_3$  edge of Ce, more specifically being interested in the X-ray Absorption Near Edge Structure (XANES). Such technique is based on the detection of the fluorescent signal emitted by the sample, created by the de-excitation processes following the absorption of the X-rays. The emitted radiation is in turn related to the absorption coefficient  $\mu$  and thus provides element-specific information about the electronic structure and the oxidation state of the sample. When detecting such radiation, it is possible to reduce the spectral broadening in the measurements by using an X-ray emission spectrometer for recording the fluorescence lines, instead of a solid state detector. At ID26 an X-ray emission spectrometer based on a five-crystal analyzer provides an instrumental energy bandwidth that is on the order of the core-hole lifetime broadening, allowing to resolve the pre-edge and the fine  $5d$  band structure of Ce, as visible in Figure 2.

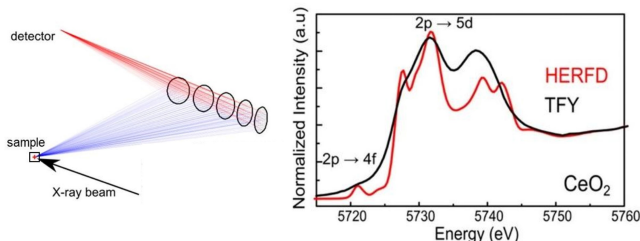


Figure 2: Comparison between Ce  $L_3$  edge spectra acquired with Total Fluorescence Yield (employing a solid-state detector) and HERFD (implementing a five-crystal analyzer at ID26) [2].

We conducted measurements on two samples of pure  $\text{CeO}_2$  (one commercially sourced and one laboratory-synthesized) and two  $\text{Pt/CeO}_2$  samples (1%Pt and 5%Pt). For each of these, four spectra were acquired under different gaseous environments (He,  $\text{H}_2$ ,  $\text{O}_2$ , and no gas), repeating the same procedure at  $50^\circ\text{C}$ ,  $200^\circ\text{C}$ , and  $300^\circ\text{C}$ . Our collaborators acquired X-ray diffraction patterns, High-Angle Annular Dark Field (HAADF) STEM images, and Selected Area Electron Diffraction (SAED) images to gain an in-depth understanding of the surface of the

$\text{Pt/CeO}_2$  samples and how Pt is displaced onto the ceria support.

## 3. Results and data analysis

HERFD measurements performed on the two pure  $\text{CeO}_2$  samples revealed that no changes were detected in the XANES spectra under the four gaseous environments and at the three different temperatures, suggesting that temperatures below  $300^\circ\text{C}$  are not enough to reduce ceria, which under  $\text{H}_2$  shows the same spectral features observed under  $\text{O}_2$  (Figure 3).

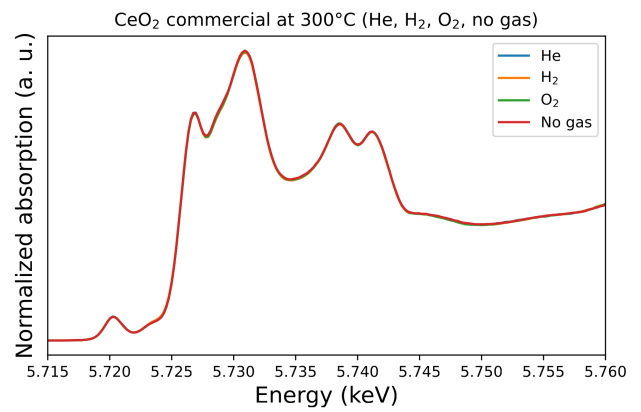


Figure 3: XANES spectra of the commercial  $\text{CeO}_2$  sample, acquired at  $300^\circ\text{C}$  under He,  $\text{H}_2$ ,  $\text{O}_2$  and no gas flow. Identical results were found for the lab synthesized  $\text{CeO}_2$  sample.

For this reason, we proceeded to analyze 1%Pt/ $\text{CeO}_2$  and 5%Pt/ $\text{CeO}_2$ . Before performing the XANES measurements, characterization studies have been carried out by our collaborators Meunier et al. [3]: XRD patterns of  $\text{Pt/CeO}_2$  reveal the presence of cubic ceria only, indicating a high dispersion of Pt, and the crystallite size of ceria particles is found to be equal to 7.4 nm. HAADF-STEM images, on the other hand, show Pt nanoparticles of sizes comprised between 0.6 and 1.5 nm on the surface of the ceria crystallites. Moreover, based on the results of their analysis, it was found that both metallic and oxidized Pt are present in comparable amounts on the surface of ca. 1 nm nanoparticles.

The HERFD-XANES spectra acquired in these cases showed that new interesting features arise. In fact, when looking at the sample with 1% of Pt, prominent changes arise at  $200^\circ\text{C}$  in the spectrum acquired under  $\text{H}_2$  flow, where a shoul-

der appears around 5.724 keV and grows even further when the temperature is increased to 300°C, as visible in Figure 4. On the other hand, for the sample with 5% of Pt it is observed that the same spectral changes appear already at 50°C, with the same shoulder growing slightly as the temperature is increased to 200°C and then 300°C (Figure 5).

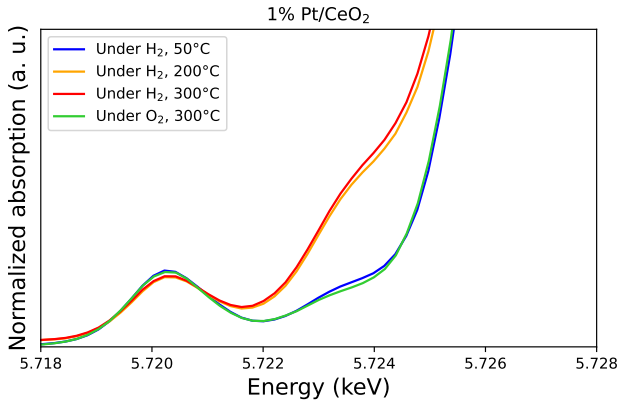


Figure 4: Magnification of the near-edge region of the 1%Pt/CeO<sub>2</sub> sample spectra acquired under H<sub>2</sub> and O<sub>2</sub> at different temperatures.

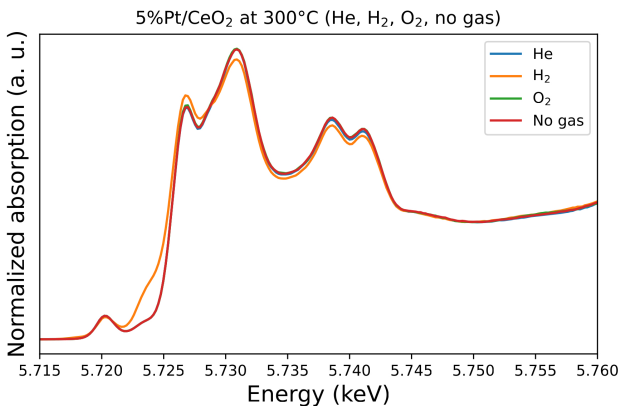


Figure 5: XANES spectra of the 5%Pt/CeO<sub>2</sub> sample, acquired at 300°C under He, H<sub>2</sub>, O<sub>2</sub> and no gas flow. Similar results were found for the 1%Pt/CeO<sub>2</sub> sample at 300°C.

## 4. Discussions

It is the first time that such spectral changes are observed in CeO<sub>2</sub>, made visible by the high energy resolution of HERFD-XANES.

We observed that going up to 300°C only allows us to see spectral changes under reduction conditions in the Pt/CeO<sub>2</sub> samples. However, as

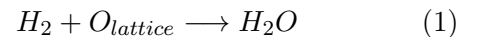
it is better discussed below, we strongly believe that such spectral modifications would appear in pure ceria as well when reaching higher temperatures, and that the presence of Pt is only able to lower the temperature at which these phenomena become visible. Therefore, we postpone to *Section 4.2* the discussion about why Pt allows to witness such spectral modifications, and we now focus on a possible explanation hidden behind the said experimental evidence.

### 4.1. The effects of oxygen vacancies on Ce electronic structure

A large shoulder around 5.724 keV is appearing when hydrogen is flown onto the sample, creating a reducing environment, while it disappears when oxygen gas flow is provided. Such spectral changes were observed in different samples and each time that the measurements were repeated, confirming the high reproducibility of the experiment and suggesting that a reversible process is at the basis of the physical explanation for the shoulder appearance.

Ceria is known for its highly mobile lattice oxygen, and we believe that such O atoms play a role into the appearance of the new spectral feature observed. In fact, we attribute the behavior shown in Figure 5 to the reduction of a fraction of Ce sites from Ce<sup>4+</sup> to Ce<sup>3+</sup>, which in turn is intrinsically related to the formation of some vacancies due to oxygen atoms leaving the lattice, a widely-investigated phenomenon in ceria.

We believe that when enough thermal energy is provided to the system, the interaction between hydrogen and the oxygen atoms from the lattice is promoted, creating water in the cell and oxygen vacancies in the ceria structure (1).



On the other hand, when oxygen is flown onto the sample, the oxygen vacancies get filled again and a configuration identical to the one prior H<sub>2</sub>-flowing is restored, as observed in Figure 5, where the O<sub>2</sub> curve is overlapping with the initial state curve (taken under He flow).

The formation of oxygen vacancies and the subsequent reduction of the surrounding Ce<sup>4+</sup> sites to Ce<sup>3+</sup> is illustrated in Figure 6. When an oxygen atom leaves its lattice position, the process of oxygen vacancy formation results in two electrons being left behind and localizing on two Ce

atoms. More specifically, the localization of such electrons occurs on the lowest-energy level available, which is the  $f$  band of Ce.

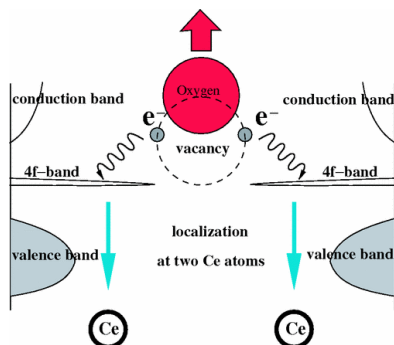


**Figure 6:** Illustration of the oxygen vacancy formation process in ceria: when the oxygen atom leaves the lattice, two electrons are localized on two Ce atoms [4].

Ceria electronic structure has generated a few controversies in the past decades, and here is reported in Figure 7 a schematic representation of Ce energy levels according to Kotani et al. [5]. A strong hybridization arises between the Ce  $4f$  and the O  $2p$  states with  $f$  symmetry around the Ce atom (here denoted as  $L$ , ligand orbital), thus Ce ground state is described by a strongly mixed state between the  $f^0$  state and the  $f^1\bar{L}$  state, where the  $f^0$  is the state with the occupied  $L$ ,  $v$  (corresponding to the O  $2p$  levels with  $d$  symmetry around the Ce atom),  $3d$  and  $2p$  levels, leaving empty the  $4f$  and the  $5d$  states, while the  $f^1\bar{L}$  has an electron located in the  $f$  band and  $\bar{L}$  represents a hole in the ligand orbital  $L$ .

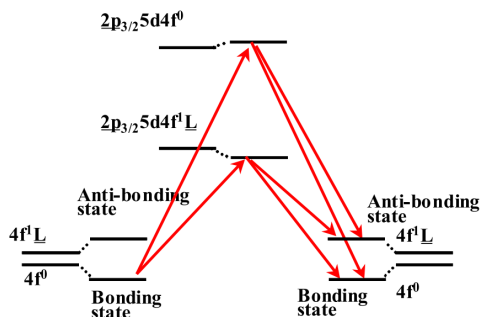


**Figure 7:** Schematic diagram of mixed valence state of Ce in  $\text{CeO}_2$ . The red arrows represent the probed  $2p_{3/2}$  to  $5d$  transitions and the four possible de-excitation paths [5].

To look at the  $L_3$  edge of Ce corresponds to

probe the Ce  $2p_{3/2}$  to Ce  $5d$  transitions, which give rise to four possible de-excitation paths. On the other hand, the pre-edge region corresponds to Ce  $2p$  to Ce  $4f$  transitions, that are quadrupole-allowed.

In general, it is challenging to treat theoretically the  $2p$  to  $5d$  excitations, where core hole screening could be the cause of strong multi-electron excitations and some dipole transitions into the  $5d$  density of unoccupied states may be left out of the calculations. The picture is therefore complicated and, to the best of our knowledge, the little shoulder around 5.724 keV has not been identified yet. However, its strong dependence on the  $\text{H}_2$  presence, *i.e.* a reducing environment, suggests that it is intrinsically related to the reduction of ceria.

For this reason, the experimental evidence observed is associated with the formation of oxygen vacancies, resulting in an increase in the Ce  $4f$  population.

This localization and delocalization of the Ce  $4f$  electron, caused by the formation and annihilation of the oxygen vacancy, is the mechanism behind the reversible reduction and re-oxidation process of cerium. This is evidenced by the reversible spectral changes that are seen when  $\text{H}_2$  is present, and disappear when  $\text{O}_2$  is present.

#### 4.2. The effects of Pt on ceria

The appearance of new spectral modifications exclusively for Pt/ $\text{CeO}_2$  systems in our experiments makes it necessary to discuss the role of ceria as a support material. The interaction between a  $\text{CeO}_2$  support and metals has been subject of many recent investigations, that reveal how the presence of a noble metal boosts the activity of  $\text{CeO}_2$  catalysts for most processes. In particular, Pt is often implemented in combinations with ceria supports in the catalysis field, meaning that a vast literature is available to understand the strong synergy arising between the two. However, it is crucial to underline that, in contrast with the vast majority of catalysis-concerning publications, our focus is turn to the support material, being the main interest of our investigation firmly on the chemical and electronic behavior of ceria.

It is known in literature that a Strong Metal-Support Interaction (SMSI) arises between the reducible support and the noble metal, leading

to three main phenomena at the interface [6, 7]. The first one concerns the electron transfer from the Pt nanoparticle to the support: in fact, when adding Pt nanoparticles onto the structure, the DOS of the CeO<sub>2</sub> support is not significantly modified, however, new available electronic states are introduced inside the bandgap, changing the HOMO and the LUMO of the system. Consequently, the very small energy difference between the highest occupied Pt states and the empty Ce *4f* allows electron transfer from the metal cluster to the support, leading to the oxidation of some Pt sites at the interface, in conjunction with the reduction of some Ce sites in its proximity.

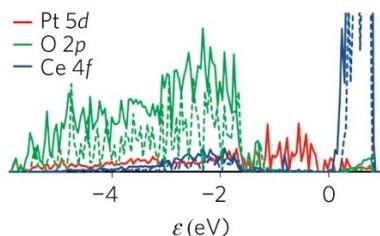


**Figure 8:** Density of states plot calculated for a pure CeO<sub>2</sub> (dashed lines) and for the Pt/CeO<sub>2</sub> system (solid line) [6].

A second phenomenon is observed only at the nanoscale: reverse oxygen spillover from the support to Pt. This corresponds to the migration of some O atoms from ceria surface to Pt, providing further reduction of the support by creating oxygen vacancies.

Lastly, in the presence of H<sub>2</sub> gas flow, Pt catalyst nanoparticles are able to dissociate H<sub>2</sub> molecules into atomic H, which then spills and diffuses onto the reducible oxide support [7].

At the same time, it is observed that Pt-O-Ce bonds are created at the interface, therefore the Ce-O bond is weakened by the presence of the metal, leading to a more reducible surface.

Similarly, the O atoms situated between Ce and Pt atom are characterized by a considerably lower energy required to remove them from the lattice, resulting in the possibility to participate in the reaction and consequently to low temperature catalytic activity [8]. Consequently, because spilled H atoms are reactive and mobile on the surface, they are able to interact with the more weakly-bounded O atoms at the lattice surface and, consequently, to reduce CeO<sub>2</sub>

at low temperature (*i.e.* below 300°C, according to our experimental observations).

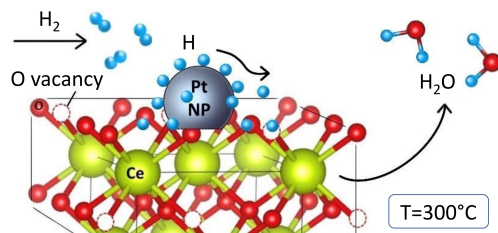


**Figure 9:** Hydrogen spillover onto the support and consequent H<sub>2</sub>O and O vacancies formation.

Therefore, at 300°C thermal energy alone is too low to trigger any significant reaction between lattice oxygen and hydrogen in pure ceria, leaving the sample not affected by the hydrogen flow, but on the contrary, when Pt is present, the kinetic barrier for the reduction of CeO<sub>2</sub> is reduced and oxygen from the CeO<sub>2</sub> lattice interacts with the H spilled onto the ceria surface, eventually forming water and leaving a vacant site in the lattice.

Moreover, we believe that the principle effect of modifying the wt % of Pt loaded onto the sample from 1% to 5% is to further reduce the reduction temperature, by an increase in PtO<sub>x</sub> species and in H atoms spilled onto the support, but we do not expect additional changes in the electronic structure of ceria. Therefore, we strongly believe that the observed spectral modifications originate from the redox properties of ceria alone, which are facilitated at lower temperature by the presence of Pt, but that do not depend on its presence in the first place.

## 5. Conclusions

Our research has demonstrated that spectroscopic techniques based on synchrotron radiation are an effective method for studying the electronic structure of Ce with the highest resolution available, providing novel insights into this intricate material. In particular, the present work stemmed from the necessity to understand how oxygen vacancy formation in the CeO<sub>2</sub> lattice affects ceria electronic structure when the sample is placed in a reducing environment. We observed that new interesting features appear when ceria is placed in a reducing environment (*i.e.* under H<sub>2</sub> gas flow), and disappear under oxidizing conditions (under O<sub>2</sub>). Such spectral

modifications were visible at temperatures below 300°C only when a small percentage of Pt was added onto the surface, accelerating ceria redox processes. In fact, we have shown that the role of platinum is to reduce the kinetic barrier for the reduction of CeO<sub>2</sub> through Pt-O-Ce bond formation and H-spillover. We attributed such reversible spectral changes to the reversible reduction and oxidation process of some Ce sites, that is in turn related to oxygen vacancy formation, since the valence change from Ce<sup>4+</sup> to Ce<sup>3+</sup> of two cations per vacancy is associated to the reversible oxygen release.

The electronic structure of the system is highly complex, making it difficult to accurately assign the shoulder observed at 5.724 keV to a specific electronic transition. To the best of our knowledge, this is the first time such a shoulder has been observed to increase *in situ* under reducing conditions. This provides new insight into the redox behavior of ceria and raises new questions in the discussion of ceria-based catalysis.

In conclusion, the redox behavior of ceria remains largely uncertain, however, the use of powerful spectroscopic techniques is providing us with a greater insight into its delicate electronic structure. Such techniques enable us to detect even the slightest changes, creating new questions and expanding our knowledge of ceria. As our understanding of the material grows, novel applications of ceria are becoming increasingly feasible.

## 6. Acknowledgements

I want to express my sincere gratitude to Professor Ghiringhelli for giving me the opportunity to experience firsthand how research is conducted at one of the largest European centers, and to Dr. Pieter Glatzel for welcoming me into his beamline. I am also deeply appreciative of all the ID26 staff for their assistance with my research and making my stay at ESRF an incredible and inspiring one, particularly Vinod who mentored me throughout my six months. I would also like to thank Luca for all the times he helped me, his Saint-Gobain collaborators for providing the samples, and Alexander and the sample environment for providing the cell.

## References

- [1] L. M. Ernst and V. Puentes. How does immunomodulatory nanoceria work? ROS and immunometabolism. *Frontiers in Immunology*, 13, 2022.
- [2] J-D. Cafun, K. O. Kvashnina, E. Casals, V. F. Puentes, and P. Glatzel. Absence of Ce<sup>3+</sup> sites in chemically active colloidal ceria nanoparticles. *Acs Nano*, 7(12):10726–10732, 2013.
- [3] F. C. Meunier, L. Cardenas, H. Kaper, Břetislav Š., M. Vorokhta, R. Grosjean, D. Aubert, K. Dembélé, and T. Lunkenbein. Synergy between metallic and oxidized Pt sites unravelled during room temperature CO oxidation on Pt/ceria. *Angewandte Chemie International Edition*, 60(7):3799–3805, 2021.
- [4] NV Skorodumova, SI Simak, Bengt I Lundqvist, IA Abrikosov, and Börje Johansson. Quantum origin of the oxygen storage capability of ceria. *Physical Review Letters*, 89(16):166601, 2002.
- [5] A Kotani, KO Kvashnina, Sergei M Butorin, and P Glatzel. Spectator and participant processes in the resonant photon-in and photon-out spectra at the Ce L3 edge of CeO<sub>2</sub>. *The European Physical Journal B*, 85:1–13, 2012.
- [6] G. N. Vayssilov, Y. Lykhach, A. Migani, T. Staudt, G. P. Petrova, N. Tsud, T. Skála, A. Bruix, F. Illas, K. C. Prince, et al. Support nanostructure boosts oxygen transfer to catalytically active platinum nanoparticles. *Nature materials*, 10(4):310–315, 2011.
- [7] W. C. Conner Jr and J. L. Falconer. Spillover in heterogeneous catalysis. *Chemical reviews*, 95(3):759–788, 1995.
- [8] W. Tang, Z. Hu, M. Wang, G. D. Stucky, H. Metiu, and E. W. McFarland. Methane complete and partial oxidation catalyzed by Pt-doped CeO<sub>2</sub>. *Journal of Catalysis*, 273(2):125–137, 2010.